

Model of adsorbate-induced missing-row reconstructions of the (110) surface of fcc metals

P. J. Kundrotas,* S. Lapinskas,* and A. Rosengren

Department of Theoretical Physics, The Royal Institute of Technology, S-100 44 Stockholm, Sweden

(Received 24 April 1997)

A microscopic model for missing-row reconstructions (MRR's), induced by atoms adsorbed in the threefold fcc hollow sites on the (110) surface of fcc metals, is proposed. The adsorbate subsystem is accounted for in the model by including interactions between dipoles, each formed by an adsorbate atom and its neighboring metal atoms. The phase diagram of the model has been calculated employing the Monte Carlo and cluster variation methods. We find overall agreement between our results and the experimental data on MRR's of fcc(110) surfaces. [S0163-1829(97)01436-7]

The (110) surface of most fcc transition metals shows a strong tendency to reconstruct, either spontaneously (Au, Pt, and Ir), or in the presence of adsorbates (Pd, Ag, Cu, Ni, Rh).¹ The rapid development of new experimental techniques, such as scanning tunneling microscopy (STM), which makes it possible to obtain atomic resolution images of surfaces, has provided a large body of information on this subject previously not available. It is well known that atoms adsorbed on the (110) surface of the fcc metals induce two main types of reconstruction depending on which kind of site available to the adsorbate atoms is occupied. If atoms are adsorbed in the so called long-bridge sites of the fcc(110) surface, the reconstruction is then either of the (2×1) added-row type with metal-adsorbate-metal chains along the [001] direction with each second row missing, or of the (2×3) paired-row reconstruction with each third row of the metal atoms in the $[\bar{1}10]$ direction missing and the adsorbate atoms being in between the paired rows. This type of reconstruction is caused mostly by nitrogen,² oxygen,³ and sometimes by other adsorbates.⁴ Another type of reconstruction is the $(1 \times n)$ missing-row reconstruction (MRR) where atoms are adsorbed in the so called threefold fcc hollow sites (hereafter for brevity called *A* sites) on the [111] microfacets of the surface, with two metal-adsorbate bonds to the top-layer and one bond to the second-layer metal atoms. In this case the rows of the metal atoms in the $[\bar{1}10]$ directions are accompanied by zig-zag chains of adsorbate atoms and each *n*th row is missing. This type of reconstruction is observed when the fcc(110) surface is covered by hydrogen⁵ or oxygen.⁶⁻⁹

There is still a lack of microscopic models which provide an understanding of the origin of this surface phenomenon. Although some simple models were proposed¹⁰ for the simplest (1×2) reconstruction on pure fcc(110) surfaces, they fail, however, to describe the more complicated adsorbate-induced fcc(110) MRR. In this paper we present a model, exploring the particular case of the oxygen-induced MRR on the Rh(110) surface which is a convenient object for theoretical studies since recent STM and low-energy electron-diffraction experiments have disclosed the changes of the surface structure with increasing amounts of adsorbed oxygen.^{7,8} The O/Rh(110) surface at oxygen coverage $c_O = 0$ shows the unreconstructed (1×1) structure and further exhibits the $(1 \times n)$ ($n = 2, 3, 4$ at $c_O = \frac{1}{2}, \frac{2}{3},$ and $\frac{3}{4}$ ML, re-

spectively) MRR's and finally at $c_O = 1$ ML the surface is again unreconstructed.⁸ One of these structures is schematically presented in Fig. 1.

The inclusion of the adsorbate subsystem in a model is usually made by using a lattice gas model of two or more interpenetrating sublattices,¹¹ but, in the case of O/Rh(110) MRR there is another possibility. Because of the asymmetric clusterlike bonding between Rh and O atoms (see Fig. 1) it is plausible to model the oxygen subsystem by assigning an effective "spin" variable $\sigma_i = \pm 1, 0$ to each "elementary fragment" of the surface composed of two *A* sites and one half of each of the neighboring top-layer Rh atoms (Fig. 2). From a physical point of view these "spins" may be interpreted as the projection on the (110) plane of the dipole moment formed by the oxygen atom together with two top-layer Rh atoms and one second-layer Rh atom. Then the Hamiltonian of our model might be written as follows:

$$\mathcal{H} = \sum_{ij} J_{ij} \sigma_i \sigma_j + \sum_{ij} K_{ij} n_i n_j + \Delta \sum_i n_i. \quad (1)$$

Here $n_i = 1(0)$ if a Rh atom occupies the surface site *i* (or not), and K_{ij} and J_{ij} are the pair interactions between the Rh atoms and the O-Rh dipoles, respectively. The chemical potential of the system, Δ , has contributions from the bulk and from external factors such as, e.g., partial pressure of the adsorbate gases. The dipole situated just below site *i* (Fig. 2) is given the same site index *i*.

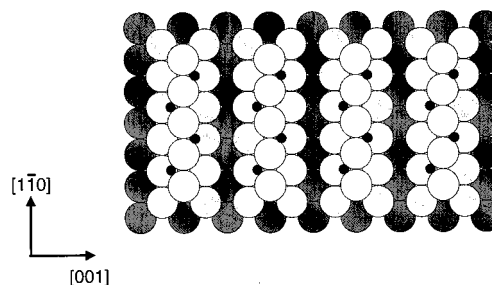


FIG. 1. (1×2) MRR on the O/Rh(110) surface. Rh atoms are shown as large open and shaded circles and small black circles denote oxygen atoms. The lighter the shade the closer to the surface the atom is.

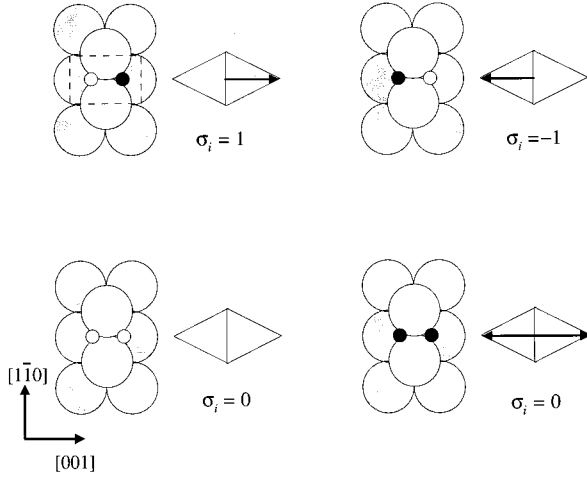


FIG. 2. The four possible arrangements of oxygen atoms over two A sites and the corresponding schematic representations of assigned dipoles. The notation of atoms is the same as in Fig. 1. A small open circle denotes an empty A site. The ‘‘elementary fragment’’ of the surface is outlined.

Long zigzag chains of adsorbate atoms imply that within an ‘‘elementary fragment’’ of the surface one (and *only one*) of the two A sites is always occupied. This allows us to exclude from consideration two of the four configurations shown in Fig. 2, namely, those with both A sites occupied or empty. Then, taking also into account that $\sigma_i = 0$ if $n_i = 0$, the relation $n_i \approx \sigma_i^2$ roughly holds and the Hamiltonian (1) can be rewritten in the form

$$\mathcal{H} = \sum_{ij} J_{ij} \sigma_i \sigma_j + \sum_{ij} K_{ij} \sigma_i^2 \sigma_j^2 + \Delta \sum_i \sigma_i^2. \quad (2)$$

The Hamiltonian (2) resembles the Hamiltonian of the so called Blume-Emery-Griffiths (BEG) model, a model originally proposed for describing phase separation and superfluid ordering in He³-He⁴ mixtures.¹² The parameter Δ in Eq. (2) controls the total number of top-layer metal atoms $\langle \sigma_i^2 \rangle \approx c_O$. An ordering at $\langle \sigma_i^2 \rangle \neq 1, 0$ exists in the model if the relation for nearest-neighbor (NN) interactions $|K_{ij}^{\text{NN}}| > |J_{ij}^{\text{NN}}|$ holds.¹³ This relation, indeed, makes sense from a physical point of view for the O/Rh(110) system assuming that the interactions J_{ij} are of dipole-dipole origin and hence should be weaker than the K_{ij} interactions of Coulomb origin which describe the correlations in the arrangements of the Rh atoms. Here, we have seemingly arbitrarily chosen $|K_{ij}^{\text{NN}}| = 3|J_{ij}^{\text{NN}}|$. Note, however, that for the topology of the phase diagram the only important point here is that $|K_{ij}^{\text{NN}}| \geq 3|J_{ij}^{\text{NN}}|$ as follows from mean-field calculations¹³ later confirmed by cluster-variation calculations.¹⁴

There are two types of ordering in the system considered. First, the Rh atoms are ordered in a chainlike manner, and, second, the zig-zag arrangement of the oxygen atoms means ‘‘antiferromagnetic’’ ordering of the O-Rh dipoles along the $[1\bar{1}0]$ direction. Moreover, the ordering of dipoles in the $[001]$ direction is of the ‘‘ferromagnetic’’ type (Fig. 1). Thus, in the notations of Eq. (2),

$$J_x^{\text{NN}} > 0, \quad J_y^{\text{NN}} < 0, \quad K_x^{\text{NN}} < 0, \quad K_y^{\text{NN}} > 0. \quad (3)$$

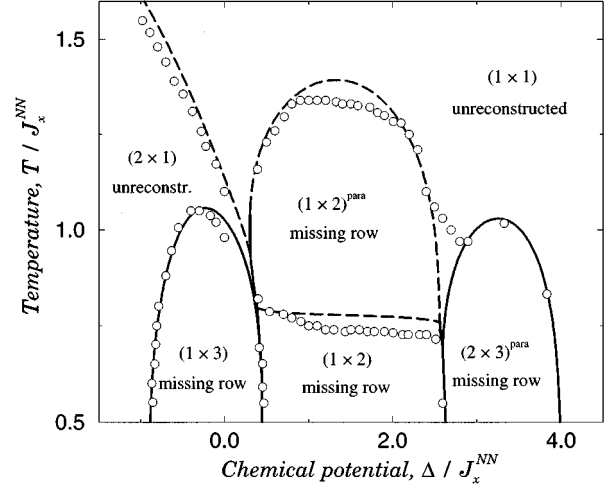


FIG. 3. The phase diagram as a function of temperature and chemical potential obtained by CVM (lines) and MC (circles) at $K_y^{\text{NN}} = -K_x^{\text{NN}} = 3J_x^{\text{NN}}$ and $K_y^{\text{NNN}} = 0.5J_x^{\text{NN}}$, $J_y^{\text{NNN}} = -0.05J_x^{\text{NN}}$. Solid and dashed lines represent the first- and second-order phase transition lines, respectively.

Hereafter the indices x and y denote $[1\bar{1}0]$ and $[001]$ directions, respectively. It should be noted that for the sake of simplicity here we restrict ourselves to the case $|J_x^{\text{NN}}| = |J_y^{\text{NN}}|$ and $|K_x^{\text{NN}}| = |K_y^{\text{NN}}|$ but the results obtained are not subject to qualitative changes with varying $|J_x^{\text{NN}}|$ and $|K_y^{\text{NN}}|$ in a wide range with respect to $|J_x^{\text{NN}}|$ and $|K_x^{\text{NN}}|$.

In order to describe the MRR’s at $c_O = \frac{2}{3}$ ML and $c_O = \frac{1}{3}$ ML interactions between the next-nearest-neighbor (NNN) Rh rows K_y^{NNN} as well as between dipoles belonging to NNN Rh rows J_y^{NNN} also should be accounted for (here we take $K_y^{\text{NNN}} = 0.5J_x^{\text{NN}}$ and $J_y^{\text{NNN}} = -0.05J_x^{\text{NN}}$). So, the model for the oxygen-induced $(1 \times n)$ MRR’s on the Rh(110) reduces to a BEG-like model on the square lattice with anisotropic NN and NNN interactions.

In order to calculate the phase diagram of the model (2) at finite temperatures T we have employed cluster-variation (CVM) and Monte Carlo (MC) methods. Technical details of the methods used can be found elsewhere (for the modified version of CVM used in the present paper Ref. 15, for MC, e.g., Ref. 16). The CVM results were obtained using a six-point basic cluster, extended in the y direction, composed of two adjacent square plaquettes. MC simulations were performed on a square lattice of typical size 42×42 with periodic boundary conditions using the Metropolis algorithm and Glauber dynamics.

The calculated (T, Δ) phase diagram is shown in Fig. 3. The (1×3) phase with stoichiometric concentration $\langle \sigma_i^2 \rangle^{\text{st}} = \frac{2}{3}$ ML shows ‘‘magnetic’’ ordering within the whole interval of existence of this phase. To the contrary, the (2×3) phase (two out of three rows of metal atoms are missing) with $\langle \sigma_i^2 \rangle^{\text{st}} = \frac{1}{3}$ ML does not exhibit ‘‘magnetic’’ ordering down to the lowest temperatures we were able to calculate. This is easily understood since, once ordering of the metal atoms is imposed by the K_{ij} ’s, the subsystem of dipoles is nothing but a system of noninteracting one-dimensional antiferromagnetic Ising chains, which, of course, does not exhibit any phase transition at finite temperatures.

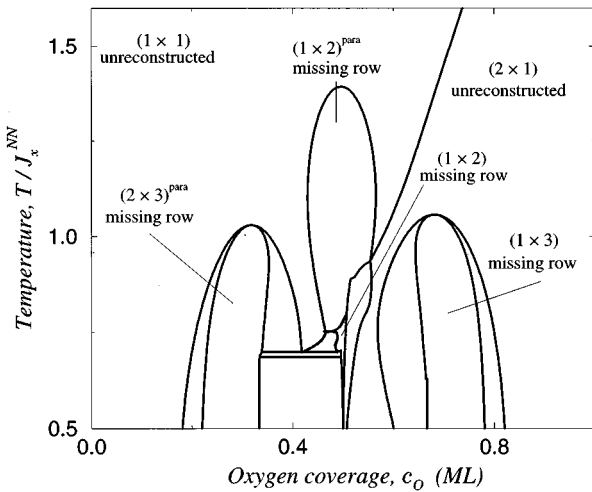


FIG. 4. The phase diagram of the O/Rh(110) surface as a function of temperature and oxygen coverage obtained by CVM. The notation of the phases and the values of interaction constants are the same as in Fig. 3. Unmarked regions represent two-phase regions between corresponding “pure” phases.

There are two kinds of the (1×2) phase in the phase diagram. At low temperatures $T/J_x^{NN} \lesssim 0.7$ “magnetic” ordering does exist while at high temperatures the “magnetic” subsystem is disordered with a preserved MRR-like ordering of metal atoms [the phase $(1 \times 2)^{para}$]. The transition line between these two phases is of the second order and is almost flat. This transition is the order-disorder phase transition of the rectangular spin- $\frac{1}{2}$ Ising model with fixed positions of spins interacting through J_x^{NN} and J_y^{NNN} . The transition temperature T_c obtained by the CVM ($T_c/J_x^{NN} = 0.775$) and MC (0.740) at $\Delta/J_x^{NN} = 1.5$ is in good agreement with the exact value (0.7413) calculated from Onsager’s equation.¹⁷

The phases (2×1) and (1×1) at their stoichiometric concentrations correspond to fully occupied and empty systems, respectively. At off-stoichiometric concentrations there are short fragments of metal rows which become longer when approaching the critical line. The only difference is that in the (2×1) phase these fragments are accompanied by the corresponding zig-zag chains of adsorbate atoms. The transition between these two phases in the limit $\Delta \rightarrow -\infty$ ($\langle \sigma_i^2 \rangle = 1$) also corresponds to the transition in the two-dimensional spin- $\frac{1}{2}$ Ising model. The value obtained by the CVM $T_c/J_x^{NN} = 2.467$ is slightly above the exact value (2.269) due to the presence of NNN interactions.

Our MC results show strong first-order phase transitions $(1 \times 2) \leftrightarrow (1 \times 3)$ and $(1 \times 2) \leftrightarrow (2 \times 3)$ with wide hysteresis in the $\langle \sigma_i^2 \rangle(\Delta)$ dependence, and $\langle \sigma_i^2 \rangle$ jumps from one stoichiometric value to another without the system being in any intermediate state. The CVM results are more complicated due to their higher resolution. They show that the system does not undergo transition directly from the (1×3) [or (2×3)] to the (1×2) phase. Instead, there are two first-order lines close to each other with unreconstructed (2×1) phase [or (1×1)] in between. The recent observation¹⁸ of a mixed phase between the (1×3) and (1×2) phases on O/Pt(110) confirms the results of our calculations.

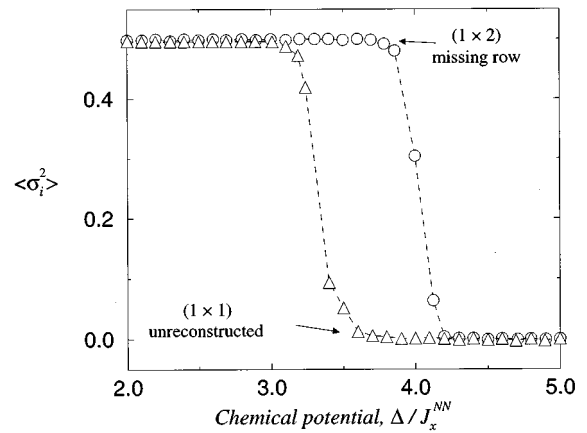


FIG. 5. The total number of particles $\langle \sigma_i^2 \rangle$ vs the chemical potential for the model (2) without (Δ) and with (\circ) the dipole-dipole interactions taken into account. The data were obtained from MC runs of 20 000 MCS/S at $T/J_x^{NN} = 0.5$ and $K_y^{NN} = -K_x^{NN} = 3J_x^{NN}$.

The (T, c_o) phase diagram (see Fig. 4) has a more complicated structure than the (T, Δ) diagram due to (i) the presence of two-phase regions instead of single first-order lines in the (T, Δ) diagram and (ii) the steep $\langle \sigma_i^2 \rangle(\Delta)$ dependence in the vicinity of some phase transitions. The (1×2) phase exists only within a narrow c_o interval around $c_o = \frac{1}{2}$ ML contrary to the wide range of Δ values for which this phase is stable (Fig. 3). This implies, that, in real experiments, the adsorbate partial pressure might change considerably but the number of atoms adsorbed on the surface would remain almost the same thereby preserving the shape of the (1×2) MRR. The phases (1×3) and $(2 \times 3)^{para}$, in turn, are found to be stable within rather wide c_o intervals. We suggest, that this explains why there are so far no experimental observations of fully ordered MRR’s at c_o between $\frac{1}{2}$ and $\frac{2}{3}$ ML, but for the O/Rh(110) system MRR’s were observed at $c_o \geq \frac{3}{4}$ ML.⁷ These phases were interpreted as $(1 \times n)$ MRR’s with $n \geq 4$.⁸ Our results, however, suggest that they are nothing but an off stoichiometric either (1×3) MRR or (2×1) phase. Indeed, for instance, islands of (1×3) MRR’s with some rows, empty at stoichiometry, and filled by Rh atoms are clearly seen in the STM image of O/Rh(110) at $c_o = \frac{3}{4}$ ML (see Fig. 2 of Ref. 7). Another simple argument confirming our point of view stems from the fact that interactions also between third- (fourth-, etc) neighboring Rh-Rh rows must be introduced in our model in order to describe the $(1 \times n)$ phases with $n \geq 4$, and this seems unreasonable from a physical point of view. A reconstructed phase with a periodicity 3 in the $[001]$ direction and with a random distribution of oxygen atoms was observed on the O/Rh(110) surface¹⁹ at $c_o = \frac{1}{3}$ ML though no clear structural model was proposed then. We believe that this observed phase is the (2×3) phase obtained in our calculations at low oxygen coverages

Thus, our model describes all MRR’s observed on the O/Rh(110) surface. Moreover the recently observed⁹ oxygen-induced (2×3) MRR on Pd(110), is an indication that our model has a general application for the adsorbate-induced MRR of the fcc(110) surface with atoms adsorbed in the A sites. It should be noted, however, that it is premature to draw quantitative conclusions about transitions temperatures

from our calculations. This would require at least one interaction constant to be known. This in turn could be determined, e. g., by comparing experimentally obtained values of phase transition temperatures with our normalized values. Unfortunately, almost all the experimental data available in the literature are obtained at room temperature only.

The large body of experimental observations shows that the zigzag fashion arrangement of the atoms, adsorbed in the A sites, is surprisingly stable depending neither on which metal exhibits the MRR of its (110) surface, nor on the kind of adsorbate atoms. This might be an indication that the dipole-dipole interactions stabilize the MRR usually not observed on pure fcc(110) surfaces (except for Pt, Ag, and Ir).

Our calculations support this point of view. We performed calculations of the $\langle \sigma_i^2 \rangle(\Delta)$ dependence for the model (2) with only NN interactions taken into account. As could be seen from Fig. 5, there is a Δ interval (in this case we consider Δ as an “external field” coming from the bulk only) where the surface remains unreconstructed if the dipole-dipole interactions are not accounted for, but with these interactions taken into consideration the surface exhibits a (1 \times 2) MRR.

This work was supported by The Swedish Natural Science Council and The Swedish Royal Academy of Sciences. P. K. is indebted to the Knut and Alice Wallenberg Foundation.

*Also at Faculty of Physics, Vilnius University, Saulėtekio 9, LT-2054 Vilnius, Lithuania.

¹S. P. Chen and A. F. Voter, *Surf. Sci.* **244**, L107 (1991), and references therein.

²For N/Rh(110) see, e.g., F. Mertens and R. Imbihl, *Lett. Nature (London)* **370**, 124 (1994); for N/Cu(110): H. Dürr, D. B. Poker, D. M. Zehner, and J. H. Barrett, *Phys. Rev. B* **49**, 16 789 (1994); for N/Ni(110): M. Voetz, H. Niehus, J. O'Connor, and G. Comsa, *Surf. Sci.* **292**, 211 (1993).

³For O/Ag(110) see, M. Canepa, P. Cantini, F. Fossa, L. Mattera, and S. Terreni, *Phys. Rev. B* **47**, 15 823 (1993); for O/Cu(110): D. J. Coulman, J. Wintterlin, R. J. Behm, and G. Ertl, *Phys. Rev. Lett.* **64**, 1761 (1990); for O/Cu₃Au(110): K. Morgenstern, H. Niehus, and G. Comsa, *Surf. Sci.* **338**, 1 (1995).

⁴For K/Cu(110) see, Ph. Hofmann, S. Bao, K.-M. Schindler, O. Schaff, M. Polčik, V. Fritzsche, A. M. Bradshaw, R. Davis, and D. P. Woodruff, *Surf. Sci.* **319**, L7 (1994); for S/Ni(110): M. Foss, R. Feidenhans'l, M. Nielsen, E. Findeisen, T. Buslaps, R. L. Johnson, F. Besenbacher, and I. Stensgaard, *ibid.* **296**, 283 (1993).

⁵For H/Cu(110) see, L. P. Nielsen, F. Besenbacher, E. Lægsgaard, and I. Stensgaard, *Phys. Rev. B* **44**, 13 156 (1991); for H/Cu(110): M. Rohwerder and C. Benndorf, *Surf. Sci.* **307-309**, 789 (1994).

⁶V. R. Dhanak, G. Comelli, G. Gautero, G. Paolucci, K. C. Prince, M. Kiskinova, and R. Rosei, *Chem. Phys. Lett.* **188**, 237 (1992).

⁷V. R. Dhanak, K. C. Prince, R. Rosei, P. W. Murray, F. M.

Leibslle, M. Bowker, and G. Thornton, *Phys. Rev. B* **49**, 5585 (1994).

⁸J. D. Batteas, A. Barbieri, E. K. Starkey, M. A. Van Hove, and G. A. Somorjai, *Surf. Sci.* **339**, 142 (1995).

⁹H. Tanaka, J. Yoshinobu, and M. Kawai, *Surf. Sci.* **327**, L505 (1995).

¹⁰J. C. Campuzano, A. M. Lahee, and G. Jennings, *Surf. Sci.* **152**, 68 (1985); M. Sandhoff, H. Pfnür, and H.-U. Everts, *ibid.* **280**, 185 (1993).

¹¹C. Uebing, *Surf. Sci.* **272**, 247 (1992); V. Bustos, G. Zgrablich, and P. Zhdanov, *Appl. Phys. A* **56**, 73 (1993); A. Patrykiejew, S. Sokółowski, T. Zientarski, and H. Asada, *Surf. Sci.* **314**, 129 (1994).

¹²F. Rys, *Helv. Phys. Acta* **42**, 606 (1969); R. B. Griffiths, *Phys. Rev. Lett.* **24**, 715 (1970); M. Blume, V. J. Emery, and R. B. Griffiths, *Phys. Rev. A* **4**, 1071 (1971).

¹³W. Hoston and A. N. Berker, *Phys. Rev. Lett.* **67**, 1027 (1991).

¹⁴S. Lapinskas and A. Rosengren, *Phys. Rev. B* **49**, 15 190 (1994).

¹⁵V. E. Zubkus and S. Lapinskas, *J. Phys.: Condens. Matter* **2**, 1753 (1990); A. Rosengren and S. Lapinskas, *Phys. Rev. B* **47**, 2643 (1993).

¹⁶*Monte Carlo Methods in Statistical Physics I*, edited by K. Binder (Springer-Verlag, Berlin, 1979).

¹⁷L. Onsager, *Phys. Rev.* **65**, 117 (1944).

¹⁸I. K. Robinson, P. J. Eng, C. Romainczyk, and K. Kern, *Surf. Sci.* **367**, 105 (1996).

¹⁹M. Bowker, Q. Guo, and R. Joyner, *Surf. Sci.* **253**, 33 (1991).